Simultaneous prediction of two independent chaotic time series using semiconductor ring lasers with optical feedback

Romain Modeste Nguimdo, Guy Verschaffelt, Jan Danckaert, and Guy Van der Sande

Abstract—We demonstrate simultaneous prediction of two independent Santa-Fe time series using a single-longitudinal mode semiconductor ring laser with optical feedback. Our results indicate that a prediction with errors comparable to the state-of-the-art can be achieved for each time series despite the two tasks are computed simultaneously.

INSPIRED by the way that the brain processes the information, computational approaches have been developed for tasks such as pattern recognition, time series prediction and classification [1], [2]. These approaches typically make use of a large number of randomly connected nonlinear nodes. With $10^2 - 10^3$ nodes, such hard tasks have been solved with acceptable errors. In a recently introduced approach, this large number of nodes has been successulfully replaced by a single nonlinear node with delay, yielding comparable performance [3]–[7].

In this contribution, we attempt to mimic another ability of the brain consisting in processing simultaneously several independent tasks. We identify semiconductor ring lasers (SRLs) as suitable devices for this purpose thanks to their capability of lasing simultaneously in two directional modes. Thus, we simultaneously predict the next sample of two independent chaotic time series.

In terms of the mean-field slowly varying complex amplitudes of the electric field associated with the two counter-propagating modes E_{cw} and E_{ccw}, and the carrier number N, the theoretical model of the SRL-based system used is :

$$\dot{E}_{cw} = \kappa(1+i\alpha)[\mathcal{G}_{cw}N-1]E_{cw} - (k_d+ik_c)E_{ccw}$$
$$+ \eta_{cw}\mathcal{F}_{cw}(t) + \sqrt{D_{cw}}\xi_{cw}(t) + k_1\mathcal{E}_1(t), \quad (1)$$

$$\dot{E}_{ccw} = \kappa(1+i\alpha)[\mathcal{G}_{ccw}N-1]E_{ccw} - (k_d+ik_c)E_{cw}$$
$$+ \eta_{ccw}\mathcal{F}_{ccw}(t) + \sqrt{D_{ccw}}\xi_{ccw}(t) + k_2\mathcal{E}_2(t), \quad (2)$$

$$\dot{N} = \gamma\left[\mu - N\left(1 + \mathcal{G}_{cw}|E_{cw}|^2 + \mathcal{G}_{ccw}|E_{ccw}|^2\right)\right], \quad (3)$$

where the parameters are the linewidth enhancement factor α, renormalized bias current μ, field decay rate κ, carrier inversion decay rate γ, feedback strengths η_{cw} and η_{ccw}, and the backscattering coefficients $k_d + ik_c$ where k_c and k_d are the conservative and the dissipative couplings, respectively. The differential gain functions are given by $\mathcal{G}_{cw} = 1 - s|E_{cw}|^2 - c|E_{ccw}|^2$ and $\mathcal{G}_{ccw} = 1 - s|E_{ccw}|^2 - c|E_{cw}|^2$ where s and c account for the phenomenological

The authors are with the Applied Physics Research Group, Vrije Universiteit Brussel, 1050 Brussels Belgium
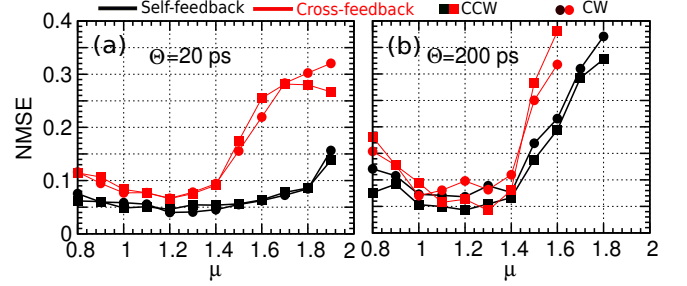
Fig. 1. NMSE for two optical inputs considering SRL with double self-feedback (black) and double cross-feedback (grey, red in color). The output is computed as $|E_{cw}|^2$ for *task* 1 and $|E_{ccw}|^2$ for *task* 2. The parameters are (a) $\Theta = 20$ ps and (b) $\Theta = 200$ ps and N=100 leading to $T_{cw} = T_{ccw} = N\Theta = 2$ ns and 20 ns, respectively. $\eta_{cw} = 10$ ns^{-1}, $\eta_{ccw} = 10$ ns^{-1}.

self- and cross-saturations, respectively. $\mathcal{F}_{cw}(t)$ and $\mathcal{F}_{ccw}(t)$ are the feedback terms. For the cross-feedback configuration, $\mathcal{F}_{cw}(t) = E_{ccw}(t-T_{ccw})e^{-i\omega_0 T_{ccw}}$ and $\mathcal{F}_{ccw}(t) = E_{cw}(t-T_{cw})e^{-i\omega_0 T_{cw}}$ where ω_0 is the solitary laser frequency, T_{cw} and T_{ccw} are delay times and $\omega_0 T_{cw}$ and $\omega_0 T_{ccw}$ are the constant feedback phases. For the self-feedback configuration, $\mathcal{F}_{cw}(t) = E_{cw}(t-T_{cw})e^{-i\omega_0 T_{cw}}$ and $\mathcal{F}_{ccw}(t) = E_{ccw}(t-T_{ccw})e^{-i\omega_0 T_{ccw}}$. The fourth terms at the RHS of Eqs. (1) and (2) represent the effect of spontaneous emission noise coupled to the CW/CCW modes. It can be explicitly written as $D_{cw,ccw} = D_m(N + G_0 N_0/\kappa)$ where D_m is the noise strength. G_0 is the gain parameter and N_0 is the transparent carrier density. $\xi_i(t)$ ($i = cw, ccw$) are two independent complex Gaussian white noises with zero mean and correlation $\langle\xi_i(t)\xi_j^*(t')\rangle = \delta_{ij}(t-t')$. The last terms in Eqs. (1) and (2) i.e $\mathcal{E}_1(t)$ and $\mathcal{E}_2(t)$ are the injected data representing different tasks to be processed in the two modes (e.g CW for *task* 1 and CCW for *task* 2), $k_{1,2}$ being the injection strengths. The original data is first convoluted with a random mask before being sent to the reservoir. The mask is generated such that it is constant over the virtual node separation Θ and periodic over one loop delay time [3], [5]. We assume data fed into the reservoir via a Mach-Zehnder modulator (MZM). Considering the convoluted data $S_{1,2}(t)$, $\mathcal{E}_{1,2}(t)$ can be written as

$$\mathcal{E}_{1,2}(t) = \frac{|\mathcal{E}_0|}{2}\left\{1 + e^{i[S_{1,2}(t)+\Phi_0]}\right\}e^{i\Delta\omega_{1,2}t} \quad (4)$$

where $\Delta\omega_{1,2}$ is the detuning between $E_{cw,ccw}$ and $\mathcal{E}_{1,2}$, $|\mathcal{E}_0|$ is the amplitude of the injection and Φ_0 is the normalized bias voltage of the MZM.

To investigate the computational ability of SRLs for parallel

Fig. 2. NMSE for SRL with (a) double self-feedback and (b) double cross-feedback configurations for different feedback strengths $\eta = \eta_{cw} = \eta_{ccw}$ considering $\Theta = 20$ ps.

processing, we consider a Santa-Fe data set of 10000 points (which is used as benchmark for prediction) in which the first 4000 points are used for *task* 1 while the last 4000 points are simultaneously used for *task* 2, meaning that the 2000 intermediate points are not considered neither for *task* 1, nor for *task* 2. By doing this, we ensure that the two tasks are independent. In each case, the first 3000 (75%) points are used for training of the readout and the remaining 1000 (25%) points are used for testing. The system performance is evaluated using the Normalized Mean Square Error (NMSE) which, for perfect prediction, is zero. We use practical parameters: $\alpha = 3.5$, $s = 0.005$, $c = 0.01$, $\kappa = 100$ ns^{-1}, $\gamma = 0.2$ ns^{-1}, $\omega_0 T_{cw} = \omega_0 T_{ccw} = 0$, $k_d = 0.033$ ns^{-1}, $k_c = 0.44$ ns^{-1}, $D_{cw} = D_{ccw} = 5 \times 10^{-6}$ ns^{-1}, $G_0 = 10^{-12}$ m^{3}s^{-1} and $N_0 = 1.4 \times 10^{24}$ m^{-3}, $k_1 = k_2 = 10$ ns^{-1}, $N = 100$ nodes, $|\mathcal{E}_0| = 2$ and $\Phi = 0$. The discrete levels of the mask for *task* 1 and *task* 2 are arbitrary set to $(0, 0.25, 0.75, 1)$ and $(-1, -0.25, 0.25, 1)$, respectively and the Santa-Fe data are rescaled so that $0 \leq S_1(t) \leq \pi$ and $-\pi/2 \leq S_2(t) \leq \pi/2$. Other parameters are set in the figure captions.

Figure 1 shows the NMSE as a function of the pump current μ for $\eta = \eta_{cw} = \eta_{ccw} = 10$ ns^{-1} and $D_{cw} = D_{ccw} = 5 \times 10^{-6}$ ns^{-1} considering a fast value of Θ (a) and relative large value of Θ (b). These values lead to the overall loop delay time of $T_{cw} = T_{ccw} = 2$ ns and 20 ns, respectively. In both cases, it is seen that, for both tasks, there is a range of the pump current for which NMSE$\lesssim 10\%$, meaning that the system can simultaneously well predict the next sample in each chaotic time series both for self-feedback (black) and cross-feedback (grey, red in color) configurations.

We further evaluate the parallel prediction performance of our system by displaying the NMSE for different values of the feedback strengths considering $\Theta = 20$ ps (Fig 2). We first decrease the feedback strength to $\eta = 5$ ns^{-1}, value for which in the absence of the input data the reservoir rest state is stable in the whole range of μ both for the cross- and the self-feedback configurations. As a consequence, NMSE$\lesssim 10\%$ is obtained for the two tasks in a broader range of the pump current ($\bullet$). However, for both configurations, it should be noticed that a further decrease of η to 1 ns^{-1} rather worsens the performance. It is interesting to note that in all cases, almost the same value of the NMSE is obtained for the two tasks. Furthermore, although the two input data are processed simultaneously, they yield similar low errors as those typically obtained when a single input data is processed [5]. This shows that, despite the two modes being coupled, the quantity of information transfered from one mode to the counter-propagating mode is not significant. Nonetheless, the results for cross-feedback configuration are slightly worse due to the fact that the two modes are coupled each other with feedback and therefore higher amount of the information is exchanged by the two modes.

We have investigated the parallel prediction abilities of semiconductor ring lasers with optical feedback. Our results have shown that although the two input data are processed simultaneously, an error characterized by NMSE as small as 0.05 can be simultaneously obtained for the two tasks. At the conference, we will also discuss the performance of the system when different types of tasks are processed simultaneously.
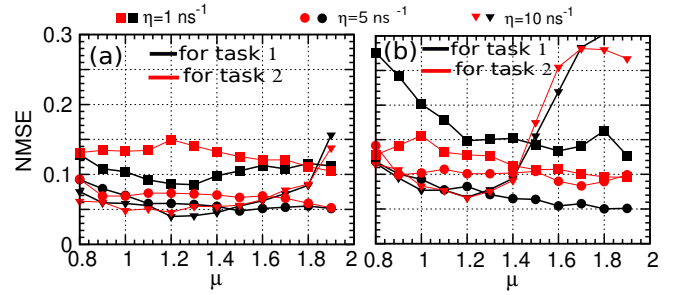
REFERENCES

[1] H. Jaeger and H. Haas, "Harnessing nonlinearity: predicting chaotic systems and saving energy in wireless communication," Science **304**, 78 (2004).

[2] A. Rodan and Peter Tiňo, "Minimum complexity echo state network", IEEE Trans. Neural Netw. Learn. Syst. **22**, 131-144 (2011)

[3] L. Appeltant, M. C. Soriano, G. Van der Sande, J. Danckaert, S. Massar, J. Dambre, B. Schrauwen, C. R. Mirasso, and I. Fischer, "Information processing using a single dynamical node as complex system," Nat. Commun. **2**, 468 (2011).

[4] L. Larger, M. C. Soriano, D. Brunner, L. Appeltant, J. M. Gutierrez, L. Pesquera, C. R. Mirasso, and I. Fischer, "Photonic information processing beyond Turing: an optoelectronic implementation of reservoir computing," Opt. Express 20, 3241 (2012).

[5] R. M. Nguimdo, G. Verschaffelt, J. Danckaert, and G. Van der Sande, "Fast photonic information processing using semiconductor lasers with delayed optical feedback: role of phase dynamics," Opt. Express **22**, 8673-8686 (2014).

[6] Y. Paquot, F. Duport, A. Smerieri, J. Dambre, B. Schrauwen, M. Haelterman, and S. Massar, "Optoelectronic reservoir computing," Sci. Rep. **2**, 287 (2012).

[7] D. Brunner, M. C. Soriano, C. R. Mirasso, and I. Fischer, "Parallel photonic information processing at gigabyte per second data rates using transient states," Nature Commun., **4**, 1364 (2013).